Supporting Information for

An Ultrasensitive Ratiometric Fluorescent Thermometer Based on Frustrated Static Excimers in the Physiological Temperature range

Sen Liang,[ab] Yuan Wang,[ab] Xueke Wu,[ab] Min Chen,[ab] Lixuan Mu,*[a] Guangwei She,[a] and Wensheng Shi*[ab]

[a] Key Laboratory of Photochemical Conversion and Optoelectronic Materials, Technical Institute of Physics and Chemistry, Chinese Academy of Sciences, Beijing 100190, China.

[b] University of Chinese Academy of Sciences, Chinese Academy of Sciences, Beijing 100049, China.

EXPERIMENTAL SECTION

Chemicals. The following chemicals were used as received: Perylene-3, 4, 9, 10-tetracarboxylic dianhydride (PTCDA, 97%) and 2-ethyl-1-hexylamine (98%) were purchased from Sigma-Aldrich. Zinc acetate ($Zn(OAc)_2$, 99.9%) and N, N'-Dimethylacetamide (DMAC, 99%) were purchased from Alfa. Methylcyclohexane (MCH, ≥99.0%) and N, N'-di(2-methyl)-3,4,9,10-perylenetetracarboxylic diimide (DM-PDI, ≥92.0%) were purchased from Aladdin. All aqueous solutions were prepared with ultrapure water (≥18 MΩ cm) and all the reagents were analytical grade.

Apparatus and Characterizations. The ^{1}H NMR spectra were recorded on a Bruker Avance 400 MHz spectrometer (Bruker Co., Germany). The UV-vis absorption spectra were recorded with a Hitachi U-4100 spectrophotometer (Hitachi Co., Japan). Temperature-sensitive fluorescence spectra were recorded with a Hitachi F-4600 spectrophotometer (Hitachi Co., Japan) and a QNW TC1 temperature controller (Quantum Northwest, inc., USA).

Synthesis of the DEH-PDI and its FSEs. The DEH-PDI was synthesized according to the previous report.[S1] In a 500 mL round-bottomed flask, 4 g (10 mmol) PTCDA, 2.9 g (22 mmol) 2-ethyl-1-hexylamine and 0.5 g $Zn(OAc)_2$ in 150 mL DMAc were stirred at 110^{o}C for 4 hours under argon atmosphere. Then 300 mL water was added and the resulting mixture was extracted with CH_2Cl_2 three times. The organic layer was dried over anhydrous sodium sulfate and evaporated. The residue was purified by silica gel column chromatography (CH_2Cl_2 as eluent) and then dried at 120°C to give the desired compound as red solid (6.1g, 93%). To fabricate the FSEs of DEH-PDI, the DEH-PDI was added into MCH to prepare the solution with various concentration (1.0×10^{-5} M, 2.0×10^{-5} M, 1.0×10^{-4} M, 1.8×10^{-4} M, 2.3×10^{-4} M, 2.7×10^{-4} M, and 3.0×10^{-4} M). After ultrasonic dissolving, the FSEs of DEH-PDI were prepared by vibrating its solutions in methylcyclohexane (MCH) at 10°C for 5h.

Calculation of the molecular electron density distribution by DFT methods. The molecular electron density distribution of DEH-PTCDI and DM-PDI was calculated by density functional theory (DFT) methods at the B3LYP/6-31G(d) level. It could be seen that both the HOMO and LUMO are localized on the polyaromatic core, and the side chains are not involved in the π-conjugation. Therefore, the two nitrogen atoms between PDI and the alkyl substitutions (2-ethylhexyl or methyl) are nodes in the π-orbital wave function. Therefore, the electron distribution of PDI would not be altered by adding the side chains.

Thermochromism measurement. The solution of DEH-PDI in MCH (C = 3×10^{-4} M) was poured into three sample bottles. The first one was stored in a refrigerator (～5°C). The second one was stored in warm water (～30°C). The third one was stored in hot water (～70°C). Ten minutes later, photographs of the three sample bottles were taken under visible light or 365 nm UV lamp. Then, all the solutions in sample bottles were poured into a test tube. After three cooling-heating cycles, the test tube was moved to a beaker with hot water. A video of the thermochromism performance in the test tube was taken.

Preparation of the microthermometer. Firstly, the micropipette was fabricated from the glass capillary (BF150-110-10) using a micropipette puller (P97, Sutter Instrument Co.). Pull parameters were heat=544, pull=0, vel=65, time=250 and pressure=500. The diameter of the tip of the micropipette is about 1.6 μm. Secondly, after the solution of DEH-PDI in MCH (C=2×10^{-4} M) was injected in the micropipette with a small syringe, the tip and end of the micropipette were sealed with epoxy.

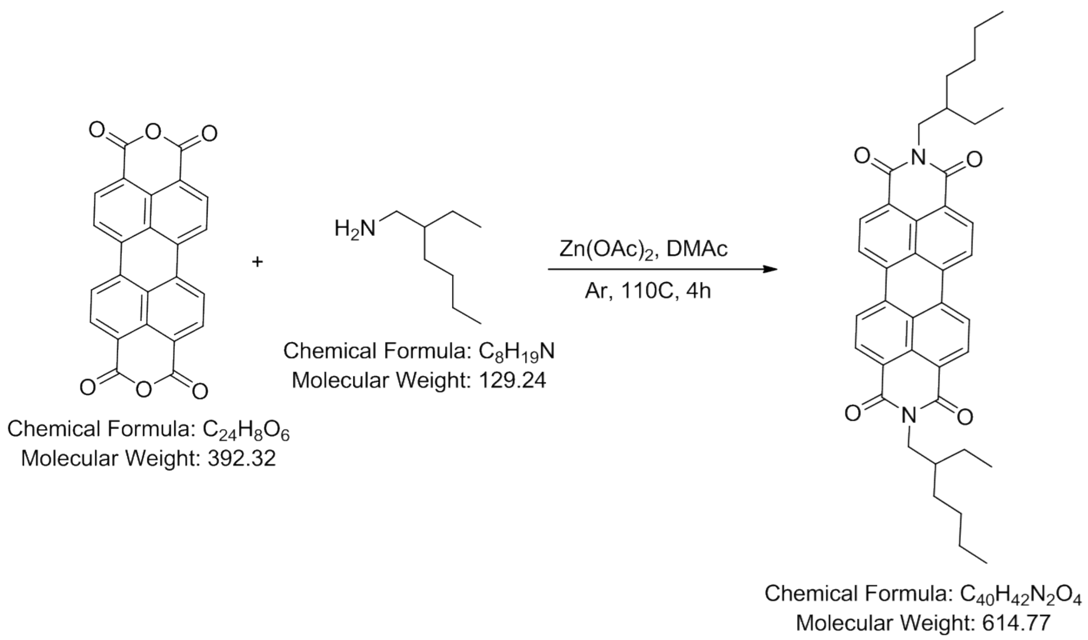

Figure S1. The synthesis of DEH-PDI.

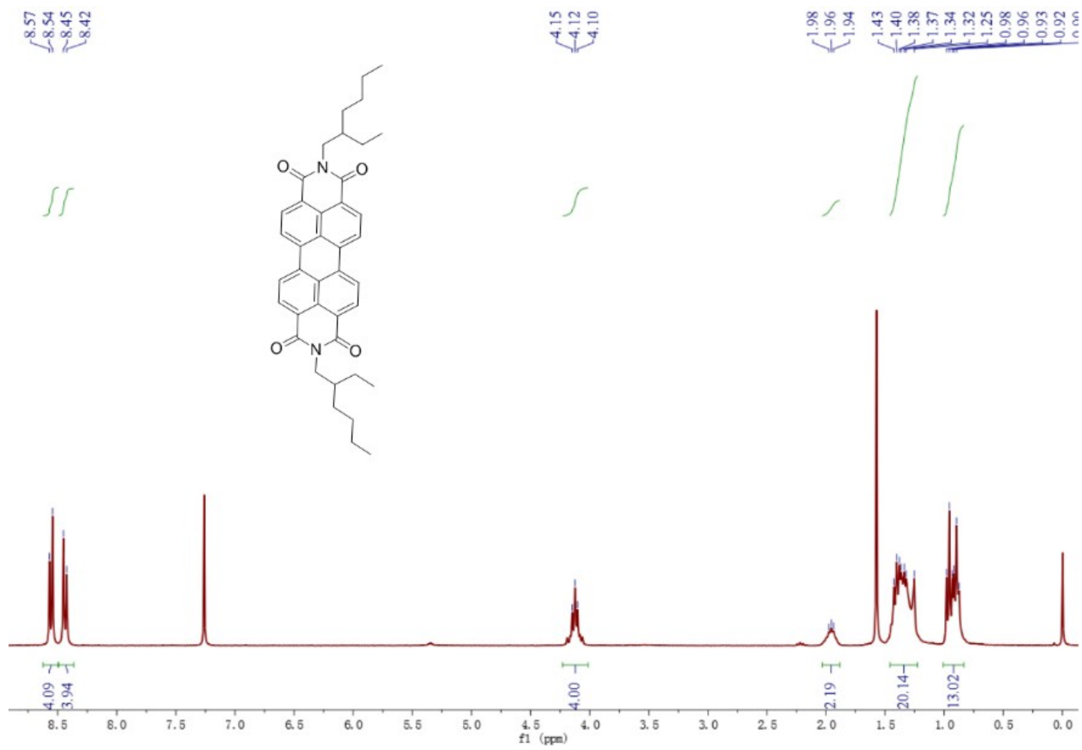

Figure S2. The ^{1}H NMR of DEH-PDI.

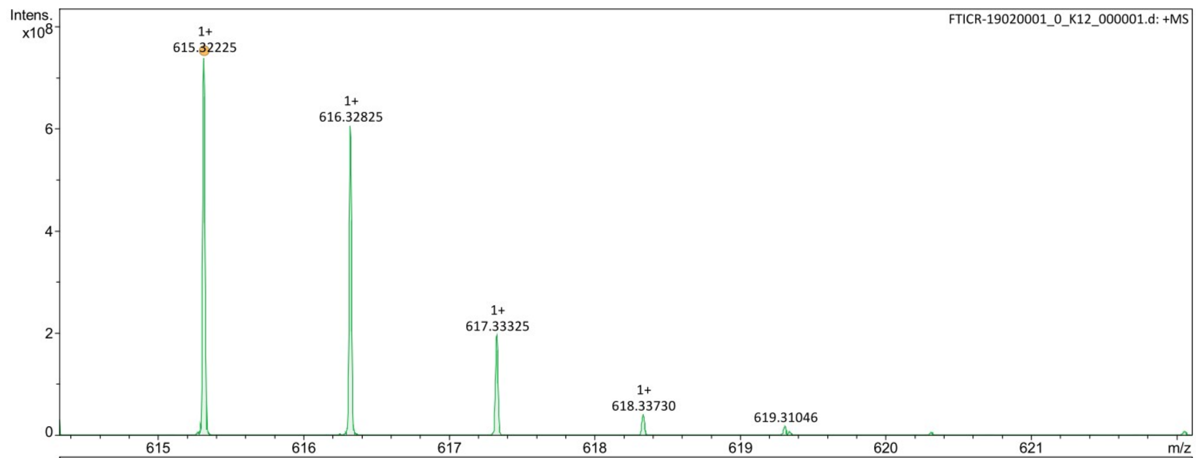

Figure S3. The MS of DEH-PDI.

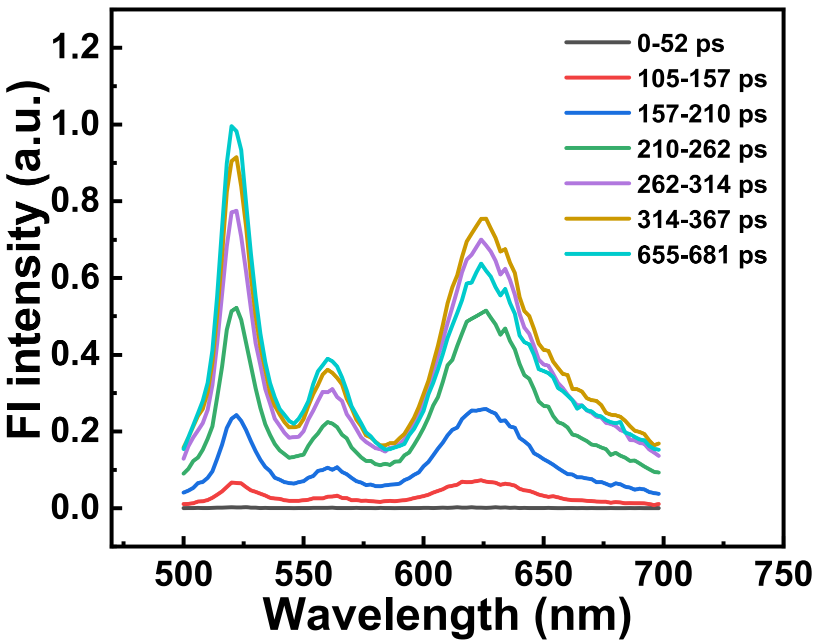

Figure S4. The time-resolved fluorescence spectra of DEH-PDI in MCH (excited at 405 nm, C=2×10^{-4} M).

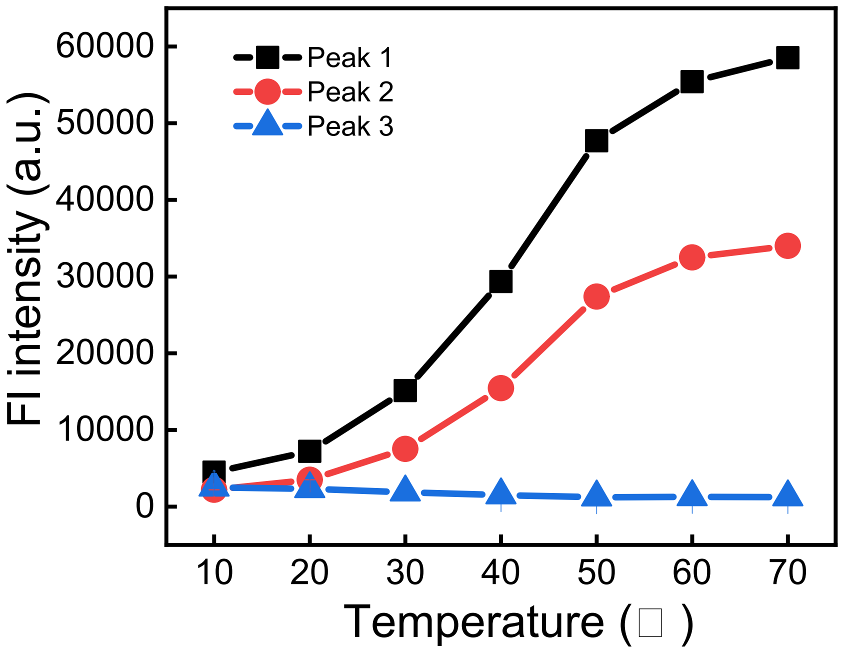

Figure S5. The fluorescence intensity of three emission peaks of DEH-PDI in MCH (C = 2×10^{-5} M, excited at 400 nm) changed with temperature.

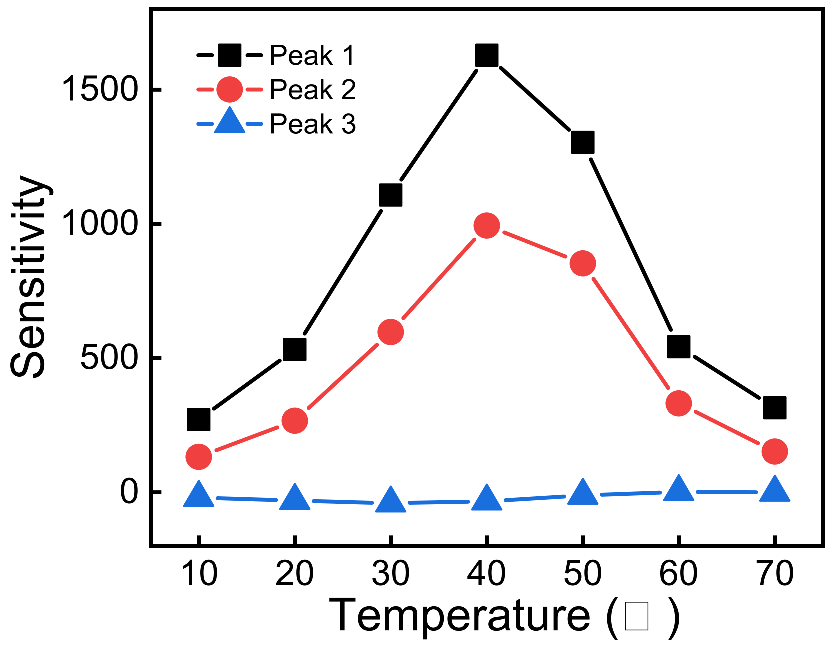

Figure S6. The sensitivities of fluorescence intensity of three emission peaks of DEH-PDI in MCH (C = 2×10^{-5} M, excited at 400 nm).

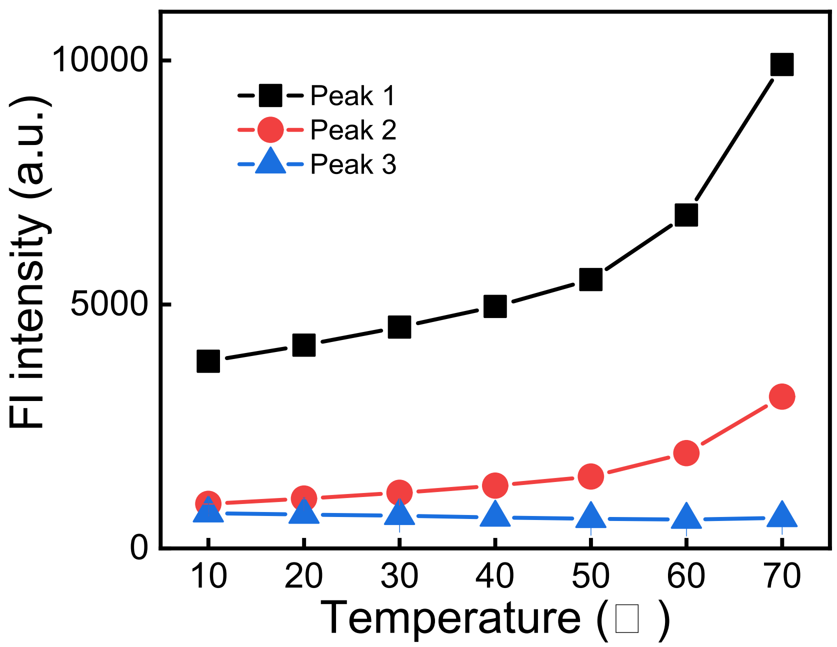

Figure S7. The fluorescence intensity of three emission peaks of DM-PDI in MCH (C = 2×10^{-5} M, excited at 400 nm) changed with temperature.

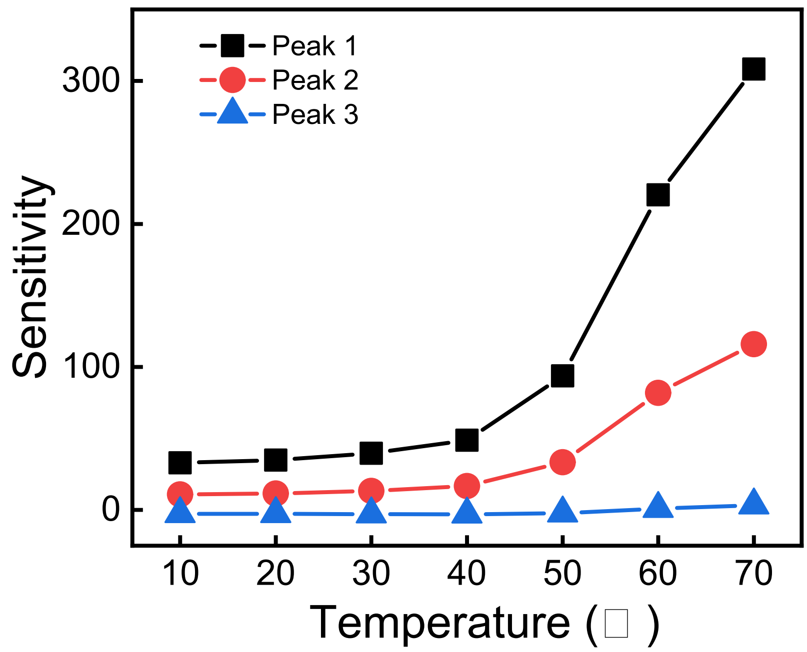

Figure S8. The sensitivities of fluorescence intensity of three emission peaks of DEH-PDI in MCH (C = 2×10^{-5} M, excited at 400 nm).

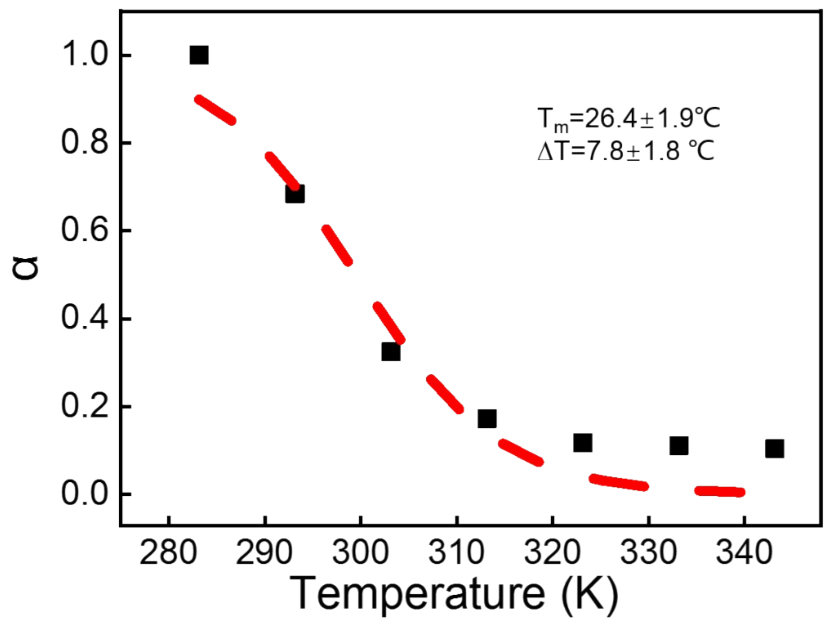

Figure S9. Normalized FSE/monomer ratio versus the temperature of DEH-PDI in MCH (C = 2×10^{-5} M, excited at 400 nm) and the fitting of T_m of DEH-PDI FSE.

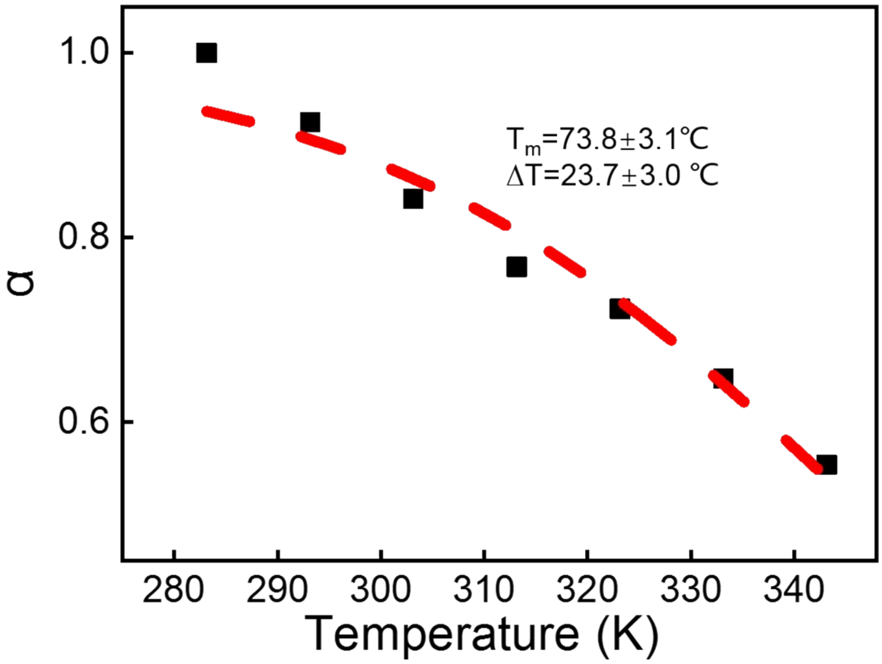

Figure S10. Normalized USE/monomer ratio versus the temperature of DM-PDI in MCH ($C = 2\times10^{-5}$ M, excited at 400 nm) and the fitting of T_m of DM-PDI USE.

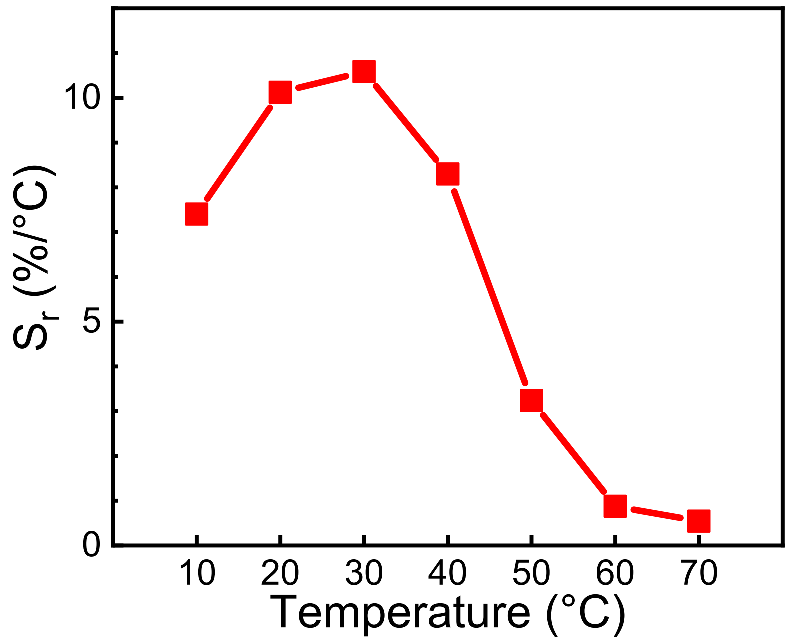

Figure S11. The relative sensitivities of the RFT based on DEH-PDI FSEs.

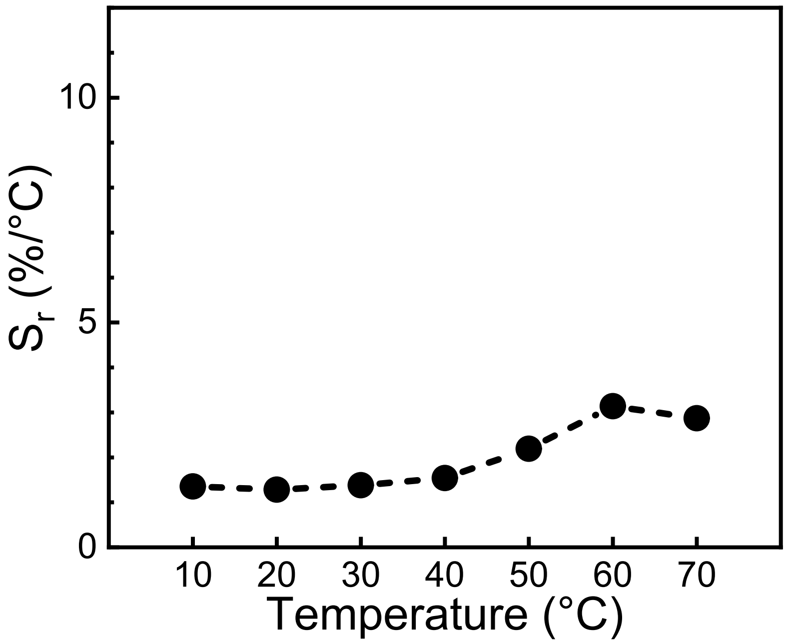

Figure S12. The relative sensitivities of the RFT based on DM-PDI USEs.

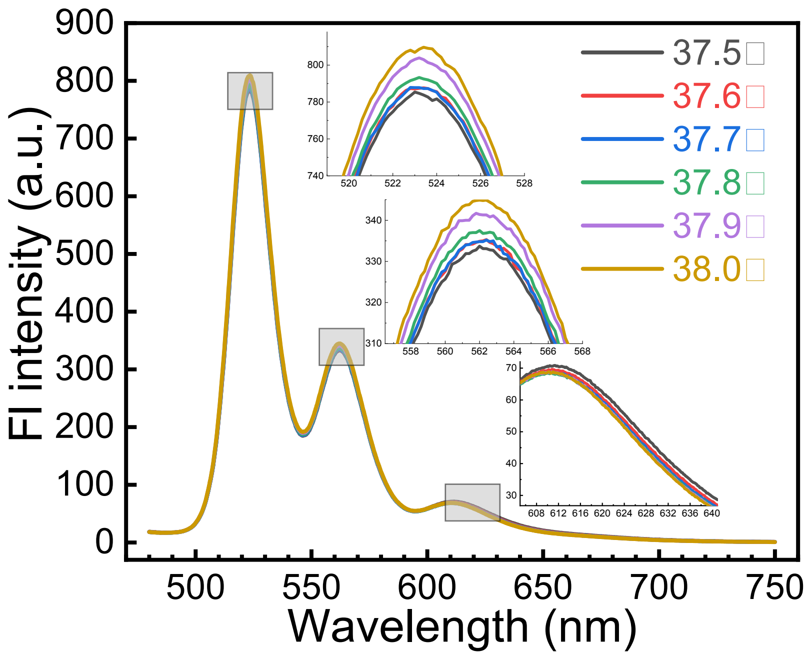

Figure S13. The fluorescence spectra of DEH-PDI in MCH (C = 2×10^{-5} M, excited at 400 nm) in the temperature range of 37.5-38.0℃.

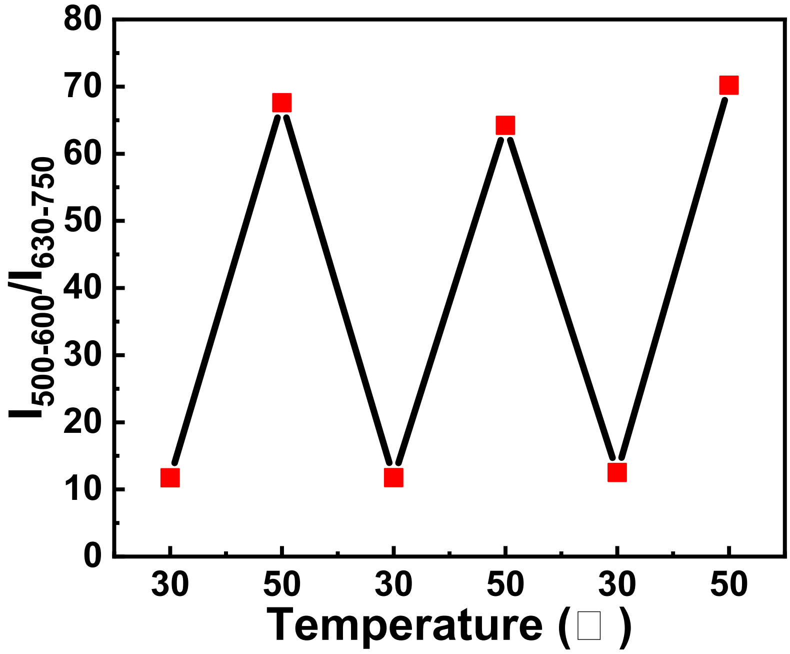

Figure S14. The reversibility test of the RFT based on DEH-PDI FSEs (C = 2×10^{-5} M, excited at 400 nm).

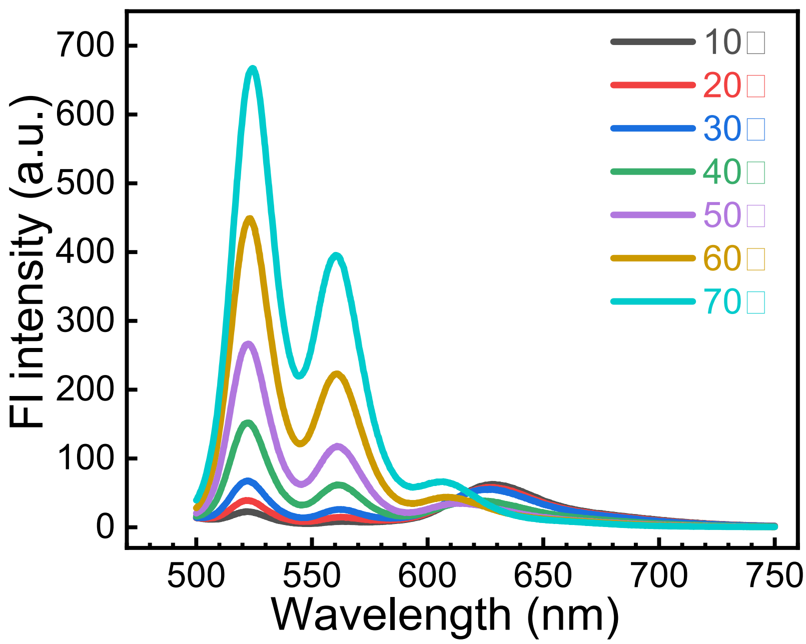

Figure S15. Fluorescence spectra of DEH-PDI in MCH (C = 3×10^{-4} M, excited at 400 nm) at different temperatures ranging from 10.00°C to 70.00°C.

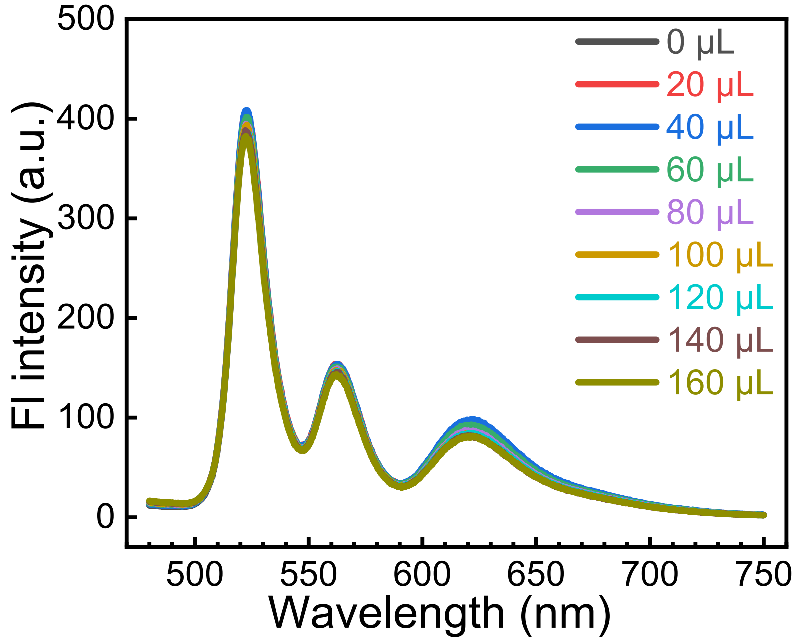

Figure S16. The influence of viscosity on the fluorescence spectra of RFT based on DEH-PDI FSEs in MCH (1mL, C = 3×10^{-4} M, excited at 400 nm) by adding viscous Tween 80.

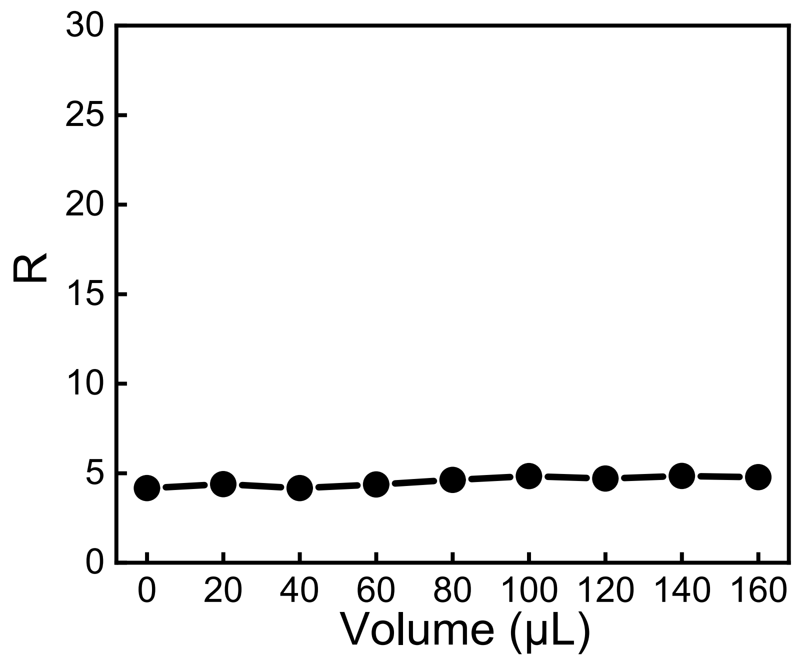

Figure S17. The influence of viscosity on the ratio values R of RFT based on DEH-PDI FSEs in MCH (1mL, C = 3×10^{-4} M, excited at 400 nm) by adding viscous Tween 80.

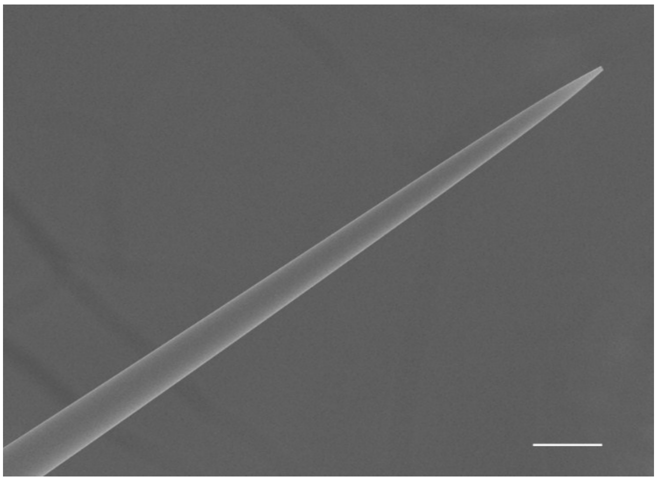

Figure S18. The scanning electron micrograph of the micropipette (scale bar is 20 μm).

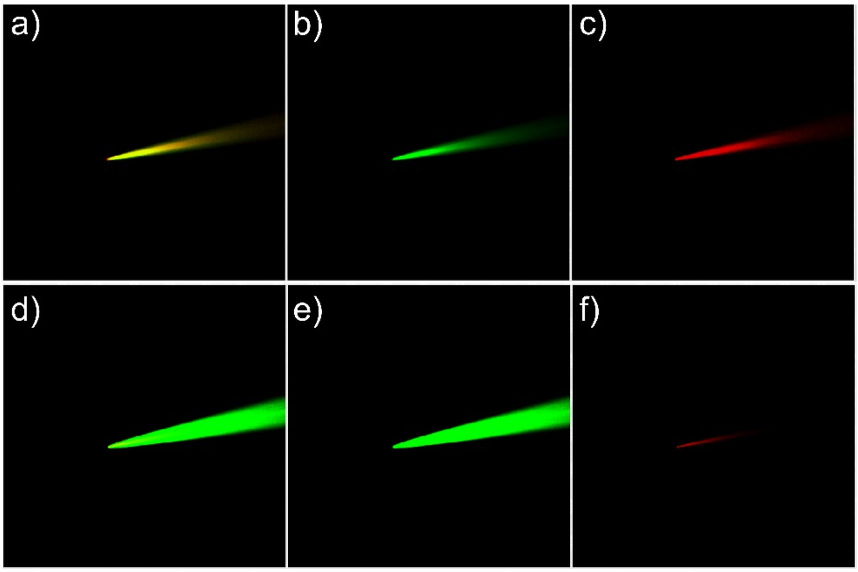

Figure S19. (a-c) Fluorescence images of the microthermometer in PBS buffer solution at 25°C: (a) merge emission (500-550 nm & 663-738 nm) (b) green emission (500-550 nm); (c) red emission (663-738 nm); (d-f) fluorescence images of the microthermometer in PBS buffer solution at 40°C: (d) merge emission (500-550 nm & 663-738 nm); (e) green emission (500-550 nm); (f) red emission (663-738 nm); λ_{ex}=405 nm, 10 mM PBS buffer solution.

Table S1 A comparison of the absolute sensitivity between our RFT and the reported ones

Material	Signal types	Temperature sensing range (°C)	Absolute sensitivity (%/°C)	Ref.
ZnO:Er^{3+} nanocrystals	Fluorescence ratio	10 – 180	0.0062	[S2]
Nanocrystals	Fluorescence ratio	22 – 97	0.83	[S3]
Core-Shell nanocrystals	Fluorescence ratio	20 – 50	4.0	[S4]
Triarylboron Compounds	Fluorescence ratio	-30 - +140	1.1 – 5.9	[S5]
N, N-dimethyl-4-((2-methylquinolin-6-yl)ethynyl)aniline	Fluorescence ratio	25 – 65	3.75	[S6]
PNIPAM	Fluorescence ratio	20 – 44	30	[S7]
Coumarin 545	Fluorescence ratio	10 – 50	0.025	[S8]
Europium MOFs	Fluorescence ratio	10 – 150	1.37	[S9]
Triarylphosphine oxide	Fluorescence ratio	-50 - +100	1.2 - 2.4	[S10]
organic films	Fluorescence ratio	-80 - +80	0.2	[S11]
FSE	**Fluorescence ratio**	**10 - 70**	**46.85 - 249.7**	**This work**

Table S2 A comparison of the relative sensitivity between our RFT and the reported fluorescent thermometers

Material	Signal types	Temperature sensing range (°C)	Relative sensitivity (%/°C)	Ref.
Perylene exciplex	Fluorescence ratio	25 – 85	~1	[S12]
Semiconducting polymer dots	Fluorescence ratio	10 – 70	~ 1	[S13]
Quantum dot/quantum rod	Fluorescence ratio	20 – 40	~ 2.4	[S14]
Lanthanide silicate	Fluorescence ratio	-261 - +177	0.1 -2.0	[S15]
MOF⊃dye	Fluorescence ratio	20 – 80	maximally up to 1.28	[S16]
Lanthanide-doped self-assembled polymer monolayers	Fluorescence ratio	23 – 65	maximally up to 1.43	[S17]
Conjugated polyelectrolytes	Fluorescence ratio	20 -70	0.99 - 2.06	[S18]
Carbon dot	Lifetime	10 – 45	1.79	[S19]
Organoplatinum metallacycles	Fluorescence ratio	-20 to 70	0.76	[S20]
Triplet sensitized upconversion	Fluorescence ratio	10 – 50	0.8 - 7.1	[S21]
FSE	**Fluorescence ratio**	**10 - 70**	**3.240 - 10.58**	**This work**

Table S3 A comparison of the precision between our RFT and the reported fluorescent thermometers

Material	Signal types	Temperature sensing range (°C)	Precision (°C)	Ref.
Nanocrystals	Fluorescence ratio	22 – 97	0.14	[S3]
Perylene exciplex	Fluorescence ratio	25 – 85	1	[S12]
Quantum Dot/Quantum rod	Fluorescence ratio	20 – 40	$\leq$ 0.2	[S14]
Lanthanide-doped self-assembled polymer monolayers	Fluorescence ratio	23 – 65	$\leq$ 0.3	[S17]
Triplet sensitized upconversion	Fluorescence ratio	10 – 50	0.1	[S21]
Nanogel	Fluorescence intensity	25 – 42	0.29 - 0.50	[S22]
Triarylboron	Max emission wavelength	-50 - +100	1	[S23]
Fluorescent polymer	Fluorescence lifetime	20 – 50	0.18 - 0.58	[S24]
Gold nanoclusters	Fluorescence lifetime and intensity	15 – 45	0.1 - 0.3	[S25]
Fluorescent nanogel	Fluorescence lifetime and intensity	20 – 40	0.02 – 0.84	[S26]
FSE	**Fluorescence ratio**	**10 - 70**	**0.04 - 0.06**	**This work**

References.

S1. S. Chen, Y. Liu, W. Qiu, X. Sun, Y. Ma and D. Zhu, *Chem Mater*, 2005, **17**, 2208-2215.

S2. X. Wang, X. Kong, Y. Yu, Y. Sun and H. Zhang, *The Journal of Physical Chemistry C*, 2007, **111**, 15119-15124.

S3. E. J. McLaurin, V. A. Vlaskin and D. R. Gamelin, *J Am Chem Soc*, 2011, **133**, 14978-14980.

S4. C.-H. Hsia, A. Wuttig and H. Yang, *ACS Nano*, 2011, **5**, 9511-9522.

S5. J. Feng, L. Xiong, S. Q. Wang, S. Y. Li, Y. Li and G. Q. Yang, *Adv Funct Mater*, 2013, **23**, 340-345.

S6. C. Cao, X. Liu, Q. Qiao, M. Zhao, W. Yin, D. Mao, H. Zhang and Z. Xu, *Chem Commun*, 2014, **50**, 15811-15814.

S7. X. Hu, Y. Li, T. Liu, G. Zhang and S. Liu, *ACS Applied Materials & Interfaces*, 2015, **7**, 15551-15560.

S8. D. Mao, X. Liu, Q. Qiao, W. Yin, M. Zhao, J. M. Cole, J. Cui and Z. Xu, *Analyst*, 2015, **140**, 1008-1013.

S9. D. Wang, Q. Tan, J. Liu and Z. Liu, *Dalton Transactions*, 2016, **45**, 18450-18454.

S10. Q. Fang, J. Li, S. Li, R. Duan, S. Wang, Y. Yi, X. Guo, Y. Qian, W. Huang and G. Yang, *Chem Commun*, 2017, **53**, 5702-5705.

S11. Q. Fang, Y. Li, Y. Wang, F. Yao, S. Wang, Y. Qian, G. Yang and W. Huang, *Journal of Materials Chemistry C*, 2018, **6**, 8115-8121.

S12. N. Chandrasekharan and L. A. Kelly, *J Am Chem Soc*, 2001, **123**, 9898-9899.

S13. F. Ye, C. Wu, Y. Jin, Y.-H. Chan, X. Zhang and D. T. Chiu, *J Am Chem Soc*, 2011, **133**, 8146-8149.

S14. A. E. Albers, E. M. Chan, P. M. McBride, C. M. Ajo-Franklin, B. E. Cohen and B. A. Helms, *J Am Chem Soc*, 2012, **134**, 9565-9568.

S15. D. Ananias, F. A. A. Paz, D. S. Yufit, L. D. Carlos and J. Rocha, *J Am Chem Soc*, 2015, **137**, 3051-3058.

S16. Y. J. Cui, R. J. Song, J. C. Yu, M. Liu, Z. Q. Wang, C. D. Wu, Y. Yang, Z. Y. Wang, B. L. Chen and G. D. Qian, *Adv Mater*, 2015, **27**, 1420-1425.

S17. M. Rodrigues, R. Pinol, G. Antorrena, C. D. S. Brites, N. J. O. Silva, J. L. Murillo, R. Cases, I. Diez, F. Palacio, N. Torras, J. A. Plaza, L. Perez-Garcia, L. D. Carlos and A. Millan, *Adv Funct Mater*, 2016, **26**, 200-209.

S18. G. H. Darwish, A. Koubeissi, T. Shoker, S. Abou Shaheen and P. Karam, *Chem Commun*, 2016, **52**, 823-826.

S19. S. Kalytchuk, K. Poláková, Y. Wang, J. P. Froning, K. Cepe, A. L. Rogach and R. Zbořil, *ACS Nano*, 2017, **11**, 1432-1442.

S20. J.-H. Tang, Y. Sun, Z.-L. Gong, Z.-Y. Li, Z. Zhou, H. Wang, X. Li, M. L. Saha, Y.-W. Zhong and P. J. Stang, *J Am Chem Soc*, 2018, **140**, 7723-7729.

S21. M. Xu, X. M. Zou, Q. Q. Su, W. Yuan, C. Cao, Q. H. Wang, X. J. Zhu, W. Feng and F. Y. Li, *Nature Communications*, 2018, **9**, 7.

S22. C. Gota, K. Okabe, T. Funatsu, Y. Harada and S. Uchiyama, *J Am Chem Soc*, 2009, **131**, 2766-2767.

S23. J. Feng, K. J. Tian, D. H. Hu, S. Q. Wang, S. Y. Li, Y. Zeng, Y. Li and G. Q. Yang, *Angew Chem Int Edit*, 2011, **50**, 8072-8076.

S24. K. Okabe, N. Inada, C. Gota, Y. Harada, T. Funatsu and S. Uchiyama, *Nature Communications*, 2012, **3**, 705.

S25. L. Shang, F. Stockmar, N. Azadfar and G. U. Nienhaus, *Angew Chem Int Edit*, 2013, **52**, 11154-11157.

S26. S. Uchiyama, T. Tsuji, K. Kawamoto, K. Okano, E. Fukatsu, T. Noro, K. Ikado, S. Yamada, Y. Shibata, T. Hayashi, N. Inada, M. Kato, H. Koizumi and H. Tokuyama, *Angew Chem Int Edit*, 2018, **57**, 5413-5417.